

Measuring the Ability of Landsat 7 to Map Vegetative Fractions Using a Near-Simultaneous AVIRIS Underflight

A. S. Warner,^{1,2} A. F. H. Goetz,^{1,2} K. B. Heidebrecht,¹ and E. L. Johnson¹

¹Center for the Study of Earth From Space (CSES)/Cooperative Institute for Research in
Environmental Sciences (CIRES),
²Department of Geological Sciences,
University of Colorado, Boulder

Contact information: Amanda Warner, University of Colorado, Boulder, Campus Box 216,
Boulder, CO 80309-0216. Email: warneras@cses.colorado.edu

1.0 Introduction

The High Plains of the United States is a 100,000 sq. km continental grain-producing region. In the last 10,000 years, following the last ice age, the sand dunes in this region have been reactivated at least four times (Muhs and Maat, 1993). These dune reactivations were caused by droughts of greater magnitude than those that caused the dust bowl in the 1930s. With the threat of warmer temperatures and drier conditions associated with global climate models, drought-like conditions can cause a decrease in natural vegetation, soil moisture, and evapotranspiration (Forman et al, 1992). Overgrazing can reduce the vegetative cover stabilizing these dunes as well. These conditions could serve to reactivate dunes currently stabilized by natural vegetation and in some areas, sandy soils that are being cultivated.

Mapping of fractional vegetative cover of less than 30% is necessary for predicting dune reactivation since it is beneath 30% vegetative cover that sand begins saltating (Pye and Tsoar, 1990; Buckley, 1987). Landsat Thematic Mapper provides a historical perspective, allowing one to study change over time. One unknown of using Landsat TM to study fractional vegetation cover in a semi-arid region is how accurately it can detect low fractions of vegetation and distinguish NPV (non-photosynthetic vegetation) from soil. Sohn and McCoy (1997) took field measurements of vegetation fractions in an arid region and compared them to mixture analysis fractions derived from their Landsat 5 data. The Landsat data consistently under-reported vegetation fractions less than 30% (Sohn and McCoy, 1997). The under-reporting of vegetation fraction can be a result of background effects from soil as well as the signal to noise ratio of the instrument (Smith, 1990). A better understanding is needed of Landsat's ability to map fractional cover in semi-arid regions.

The study undertaken in this paper is to compare the ability of Landsat 7 data to map cover types on the High Plains using AVIRIS as a baseline. We applied spectral mixture analysis methods to arrive at fractions of cover for both Landsat 7 and AVIRIS using AVIRIS endmember bundles for the unmixing.

2.0 Methods

2.1 Site Description

The AVIRIS lines used in this study include sections of the Ft. Morgan Dune Field in northeastern Colorado (See Figure 1). The Ft. Morgan dune field, as well as other major dune formations in Colorado, and the High Plains are formed by prevailing northwest winds (Stokes and Swinehart, 1997). The Morgan County dunes are parabolic or compound parabolic dunes with arms pointing upwind that can be up to several kilometers long (Forman et al, 1992). Vegetation is usually thickest on the lower slopes and sparse to absent near the nose of the dunes (Pye and Tsoar, 1990).

2.2 AVIRIS Lines

The AVIRIS data were collected on July 10, 1999 beginning at 10:04 am MDT. The Landsat 7 scene corresponding to this area was collected at 11:30 am MDT. The line used in this study is eight and a half degrees off of the solar principal plane—resulting in minimal BRDF effects. The northeast-southwest trending flight line is

51 degrees off of the principal solar plane, and analysis of these data has shown significant BRDF effects in the forward scattering direction. The soil calibration site, however, is in the center of this line where BRDF effects should be minimal.

Ft Morgan Dune Field

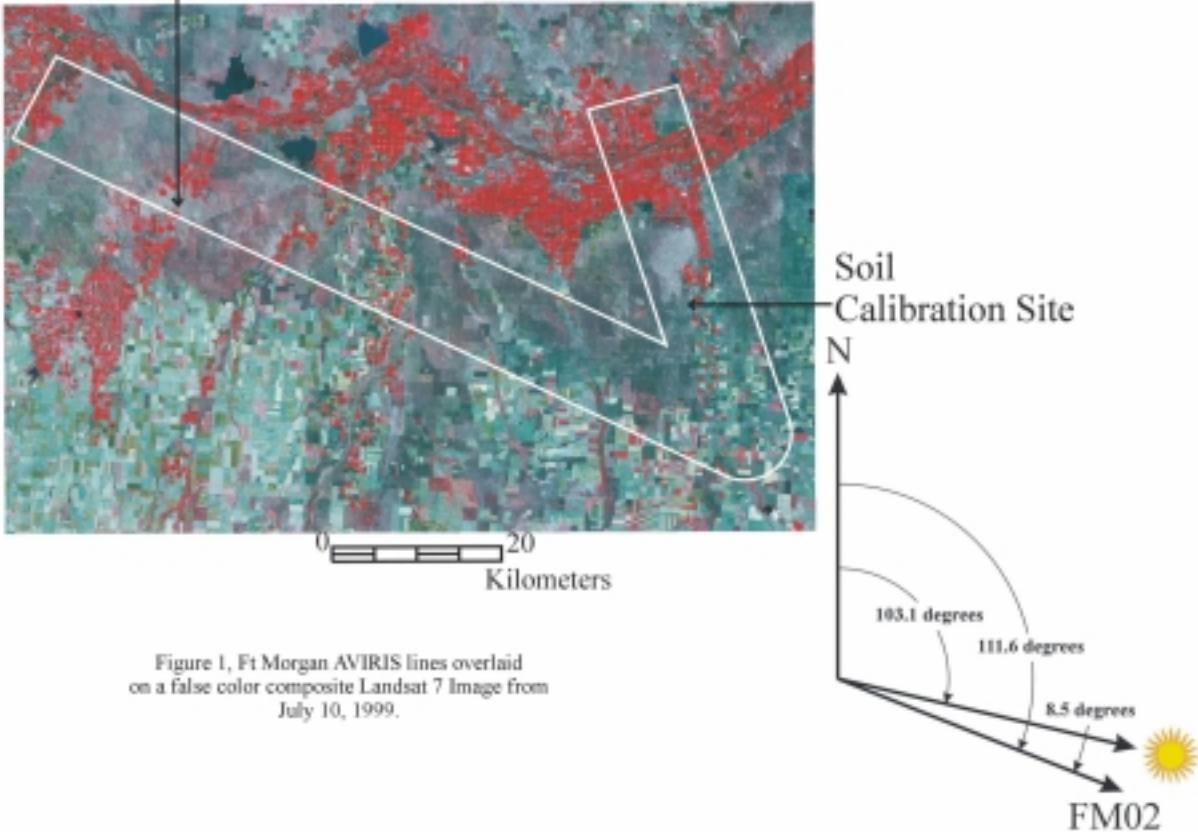


Figure 1, Ft Morgan AVIRIS lines overlaid on a false color composite Landsat 7 Image from July 10, 1999.

2.3 Atmospheric Correction

ATREM was performed on the AVIRIS data to remove atmospheric scattering and absorption features (Gao et al, 1993). Field spectra of bare soil were acquired at the Wager's farm near Brush, Colorado with an ASD Field Spectrometer (See Figure 2). The mean soil field spectrum was used as a ground correction to remove systematic and modeling errors from the resulting ATREM reflectance values. The Landsat 7 data were atmospherically corrected by performing a dark object subtraction (Chavez, 1996) followed by a ground calibration with the mean soil field spectrum convolved to Landsat 7 bandpasses.

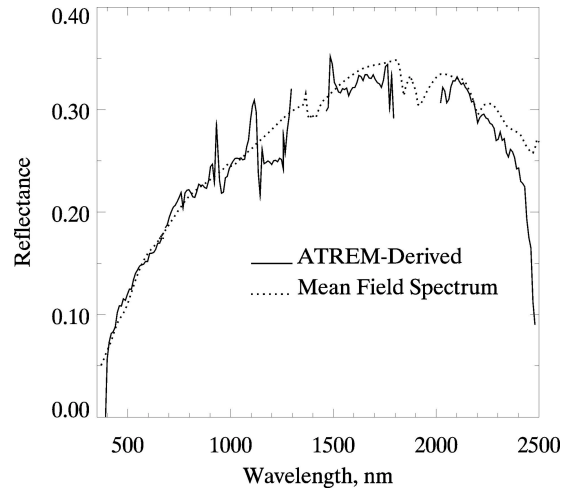


Figure 2. Mean soil field spectrum used in the atmospheric correction of the AVIRIS and Landsat 7 data.

2.4 Georegistration and Data Preparation

In order to make the AVIRIS scene used in this study comparable to the Landsat 7 area, the AVIRIS data had to be geocorrected. These data were acquired on the ER-2 aircraft and there was significant pitching. This year, the ER-2 had a GPS-INS mounted on-board. With the data collected from the GPS-INS, precise location of each pixel can be achieved. The Boardman Algorithm for geocorrection utilizes these data in “moving” pixels to the proper spatial location (Boardman, 1999). The AVIRIS data, once corrected, were warped to Landsat 7 geocorrected imagery for better agreement using nearest neighbor resampling to best preserve the radiometry of the AVIRIS data. The Landsat 7 data were resampled to match the 17.2 meter pixels of the AVIRIS data. This was done to preserve the integrity of the AVIRIS data since they are the basis of comparison in this study.

The endmembers were selected using ENVI’s Pixel Purity Index following a Minimum Noise Fraction transformation (Boardman and Kruse, 1994). The purest pixels were input into N-dimensional visualization and endmembers were selected from the corners of the simplex (Boardman, 1993). Pure spectra were grouped into green vegetation, NPV, and soil bundles. Spectra that were obvious mixtures were not used in this study, i.e., spectra that clearly have a green vegetation signature yet in the region beyond 2.0 μm (SWIR2) have a clay absorption feature. See Figure 3 for sample soil and green vegetation AVIRIS spectra convolved to Landsat 7 bandpasses. See Figure 4 for a plot of AVIRIS endmember bundles and AVIRIS endmember bundles convolved to Landsat 7 bandpasses.

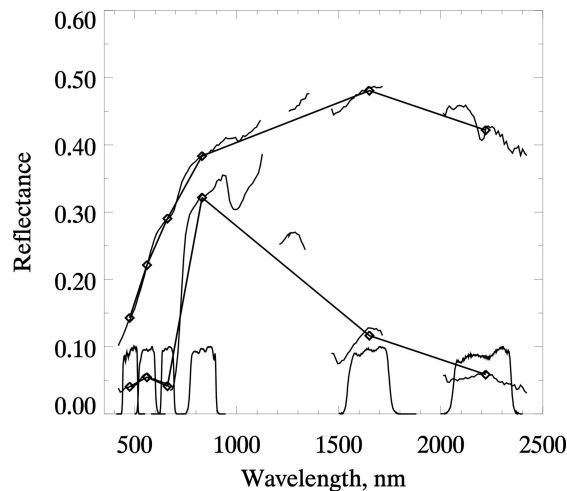


Figure 3. Landsat 7 filter response functions and spectrally resampled spectra.

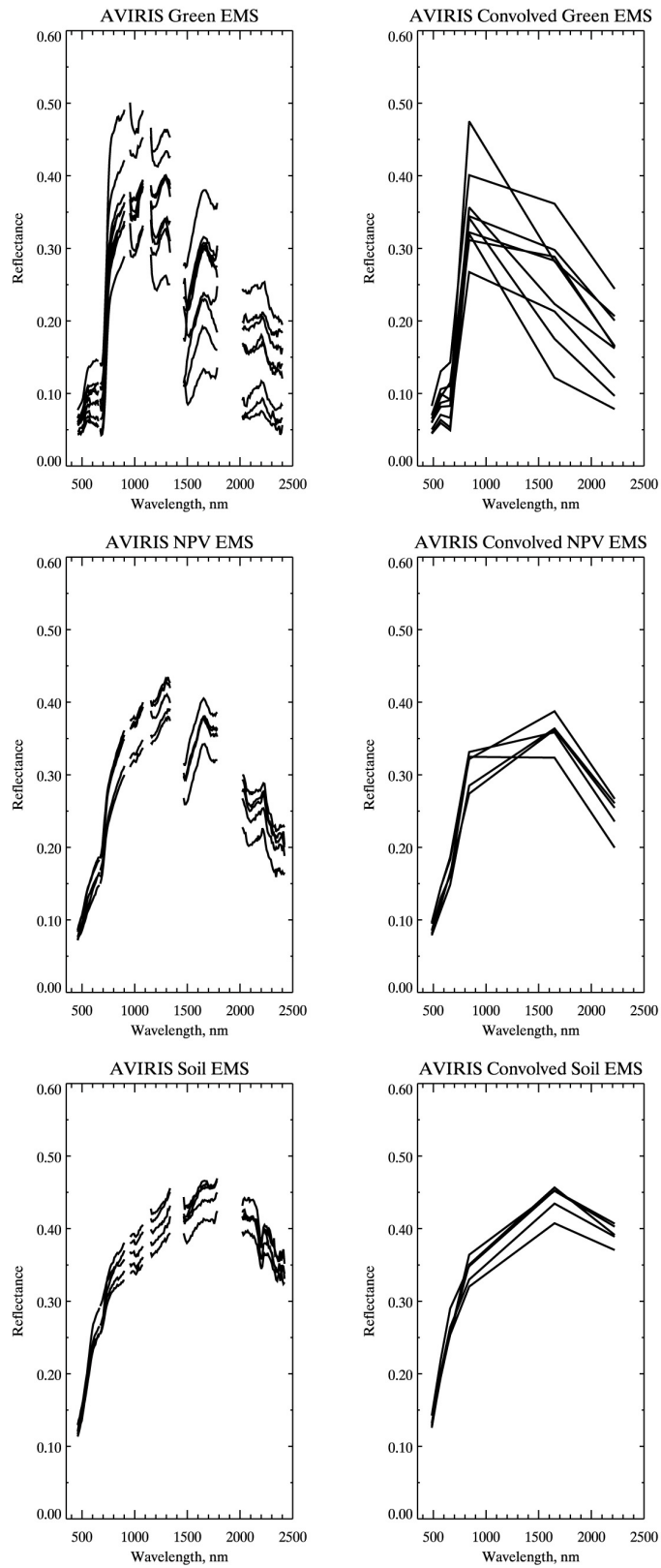


Figure 4. AVIRIS endmembers (EMS) on the left and AVIRIS endmembers convolved to Landsat 7 bandpasses on the right.

2.5 AutoSWIR and AutoSMA

AutoSWIR and AutoSMA are methods developed by Asner and Lobell (2000, in press) and Asner et al (in review), respectively, that incorporate the Monte Carlo algorithm in selecting endmember combinations to unmix on the pixel level. AutoSWIR concentrates on the 2100-2400 nm (SWIR 2) region of the solar reflected spectrum as the differences in the physical properties of surface materials, i.e., green vegetation, soil, and NPV, are more distinguishable from one another in this region. This method uses field-collected spectra “tied” to one wavelength to minimize albedo variations.

Unmixing with AutoSWIR and AutoSMA is unconstrained linear spectral unmixing with a Monte Carlo approach to maximize the incorporation of endmember variability in a given pixel. Bateson et al (1998) explains that the inherent variability in vegetative canopies makes unmixing a pixel with a single endmember spectrum often prone to error. Both AutoSWIR and AutoSMA make use of endmember bundles to better encompass the variability of natural surfaces.

2.6 Application of AutoSMA

The process used in this study, AutoSMA, was developed by Asner et al (in review) for better applicability to Landsat data. It differs from the AutoSWIR method in that it uses full spectrum linear unmixing instead of only using SWIR 2 tied spectra. The Monte Carlo approach and the incorporation of endmember bundles is still used in this algorithm. The application of this method to this study is described below:

- Full spectrum endmembers of each cover type are selected from the AVIRIS imagery and are grouped into bundles.
- The algorithm randomly selects endmember combinations from the bundles.
- The algorithm performs unconstrained linear spectral mixture analysis and computes a fractional cover for each endmember for a given pixel for a given run.
- Upon the completion of a user-defined number of runs, a mean cover fraction is computed for each cover type.
- A standard deviation is also computed for each cover type based on the range of fractions computed for each pixel.
- The process is repeated with AVIRIS endmember bundles convolved to Landsat 7 bandpasses.

3.0 Results

3.1 Comparison

Upon the completion of unmixing both sub-scenes, regions of interests were selected and mean and standard deviation values were taken for these regions. Since the AVIRIS data have been georectified, these regions can easily be moved between the images. As shown in Figure 5, all fractions are well correlated with very high R^2 values. The fractions derived with AVIRIS bundles convolved to Landsat 7 bandpasses have slightly larger standard deviations, but the value computed with the AVIRIS data lies within this range. The soil fractions have the smallest standard deviation of all the cover types, which can be attributed to the relative similarity of the spectra in the endmember bundle, since one soil type dominates this sub-scene (USDA, 1968). The different “pure” soil spectra from this scene are associated with differences in topography and lack of completely bare soil regions in this scene, meaning a small contribution of other cover types to the soil spectra.

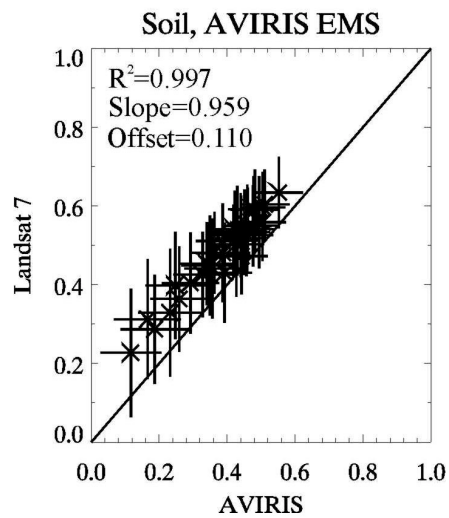
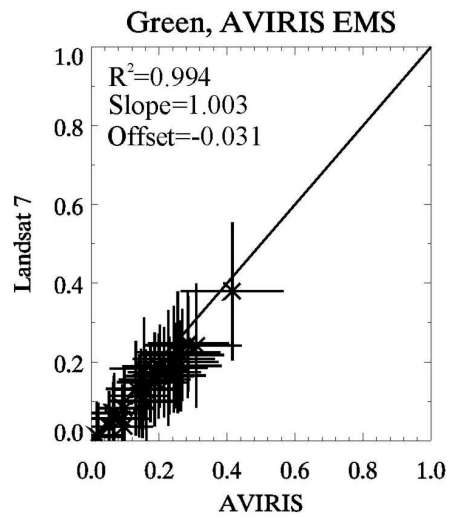
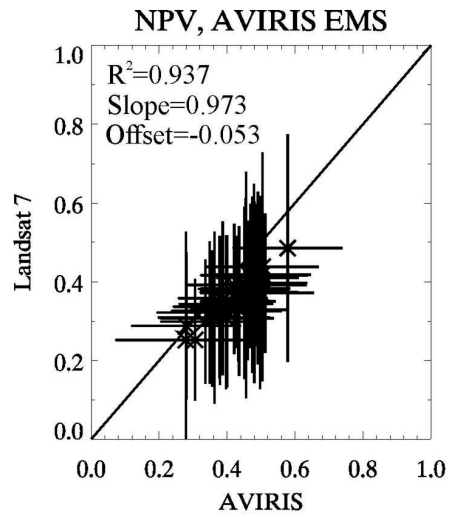


Figure 6. Cover fractions derived from Landsat 7 and AVIRIS data. Landsat 7 fractions are on the y-axis and AVIRIS fractions are on the x-axis.

3.2 Recombination Spectra

For each run in Monte Carlo Unmixing, a mean is computed for each of the randomly selected cover types. By inverting this process, i.e. multiplying the endmember selected by the fraction computed for each run, summing the fractions together and taking the resulting mean recombination spectrum, the results can be compared to the original spectrum. While recombining spectra does not necessarily yield a unique answer, it is a good indicator that the algorithm is functioning properly and the resulting fractions are feasible (See Figure 7).

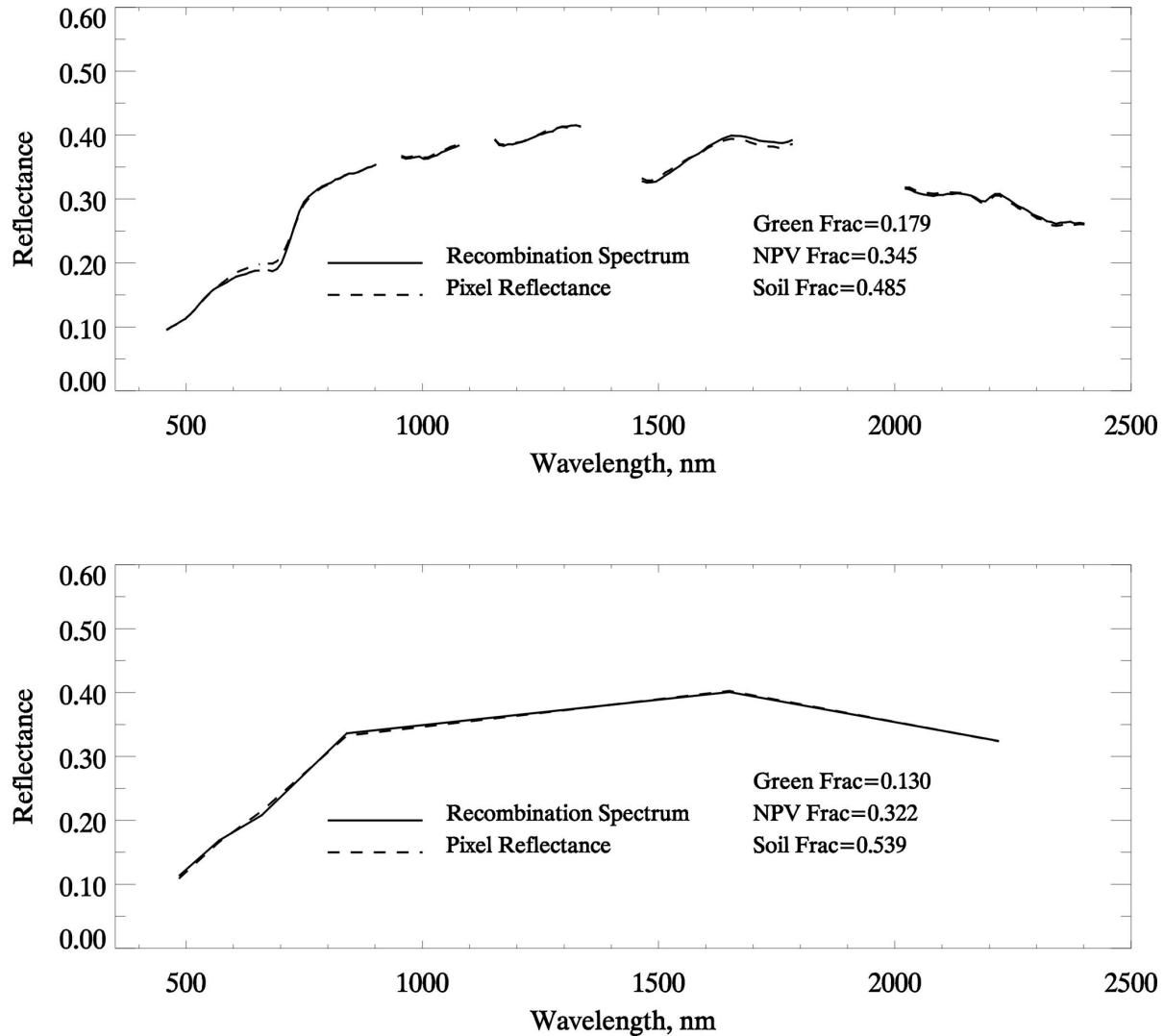


Figure 7. AVIRIS and Landsat 7 recombination spectra.

4.0 Discussion and Conclusions

4.1 Performance of Monte Carlo Unmixing

One of the advantages of Monte Carlo Unmixing is achieving mathematically feasible results with less experimentation to find the proper endmember combination. Though the dimensionality of the data is $n+1$, n being number of bands with coherent eigen images, there certainly exist many more substances on the ground than can ever be contained in the dimensionality of an image. By incorporating multiple endmember unmixing, whether the spectra come from libraries, field data, or are image derived, there is an advantage over trying to unmix an area with a limited group of endmembers (Roberts et al, 1998). When trying to unmix a region with a specific number of

endmembers, there is the possibility that one of the endmembers may not exist in a pixel. If the substance does not exist then a negative fraction is returned. Constrained mixing, while producing results within the feasibility constraints, gives a false impression of what is present in a pixel, since fractions are being forced to be equal to one. By randomly creating endmember combinations, the inherent variability of an image pixel is more effectively taken into consideration. The algorithm significantly cuts down on the time needed to determine the best endmember combination for a pixel.

4.2 Using AVIRIS Derived Endmembers to Unmix Landsat 7 Data

Landsat imagery has only six bands coinciding with the range of AVIRIS. The maximum number of dimensions that can be seen in Landsat data is seven. The number of endmembers able to be uniquely distinguished is related to the number of dimensions. There are many more substances that are spectrally unique enough to be called endmembers in AVIRIS data and still more may exist. The incorporation of bundles in this method maximizes endmember variability since the resulting reflectance of a pixel is the result of interactions between soil, NPV, and green vegetation (van Leeuwen and Huete, 1996). The unmixing being performed with both sensors is only with three endmembers at a time. The solution for endmembers is underdetermined with both sensors. With AVIRIS having a higher spatial and spectral resolution than the Landsat instruments, we can say that although we cannot find these substances in Landsat data, they still exist. By using the AVIRIS endmembers to unmix the Landsat data, the same reference points are used and the resulting fractions are directly comparable.

4.3 Conclusions

Soil cover fractions for the Landsat and the AVIRIS data are very well correlated and have the smallest standard deviation of the cover types. The fractions of green vegetation and NPV correlate well between AVIRIS and Landsat 7, but the Landsat 7 fractions have larger standard deviations and are less precise. The AutoSMA procedure produces results that are within the feasibility constraints for both sensors. The algorithm is fast and efficient in maximizing endmember variability and arriving at a plausible result.

Incorporating AVIRIS spectra adds spectral leverage to the Landsat data. There is a baseline for comparing the two sensors and determining Landsat 7's performance using the AVIRIS data as a proxy for the gaps in Landsat 7's spectral range. Preliminary results of unmixing Landsat 7 with Landsat 7-derived endmember bundles looks promising, but more work is needed to verify the consistency of Landsat 7 unmixing results.

5.0 Acknowledgements

The authors wish to thank Greg Asner for his software and helpful comments in this endeavor as well as the entire AVIRIS team for accommodating our flight and data requests—without their help none of this work could be done. Special thanks to Joe Boardman for his assistance with geocorrection. Thanks to Anne Bateson for helpful comments.

This work is supported by NASA/GSFC under contract number NAG5-3437.

6.0 References

- Asner, G. P. and D. B. Lobell, 2000, "A biogeophysical approach for automated SWIR unmixing of soils and vegetation," *Remote Sensing of Environment*, in press.
- Asner, G.P., et al, in review, "Land-use change analysis in the Amazon Basin using Landsat TM and Monte Carlo unmixing".
- Bateson, C. A., et al, 1998, "Incorporating endmember variability into spectral mixture analysis through endmember bundles", 1998 Proceedings from the Airborne Geosciences Workshop.
- Boardman, J. W., 1993, "Automated spectral unmixing of AVIRIS data using concept geometry concepts", 1993 Proceedings from the Airborne Geosciences Workshop:11-14.
- Boardman J.W., and F.A. Kruse, 1994, "Automated spectral analysis: A geological example using AVIRIS data, North Grapevine Mountains, Nevada", Proceedings of the Tenth Thematic Conference on Geologic Remote Sensing, Volume 1: I409-I418.
- Boardman, J. W., 1999, "Precision geocoding of Low-Altitude AVIRIS data: Lessons learned in 1998", 1999 Proceedings from the Airborne Geosciences Workshop.

- Buckley, R., 1987, "The effect of sparse vegetation on the transport of dune sand by wind", *Nature* 325: 426-428.
- Chavez, P. S., 1996, "Image-based atmospheric corrections revisited and improved," *Photogrammetric Engineering and Remote Sensing* 62, 1025-1036.
- Forman, S. L., Goetz, A. F. H., and Yuhas, R. H., 1992, "Large-Scale stabilized dunes on the High Plains of Colorado: Understanding the landscape response to Holocene climates with the aid of images from space", *Geology* 20: 145-148.
- Gao, B., Heidebrecht, K. B., and Goetz, A. F. H., 1993, "Derivation of scaled surface reflectances from AVIRIS data", *Remote Sensing of Environment* 44: 165-178.
- Muhs, D. R., and Maat, P. B., 1993, "The potential response of eolian sands to greenhouse warming and precipitation reduction on the Great Plains of the USA", *Journal of Arid Environment* 25:351-361.
- Pye, K., and Tsoar, H., 1990, *Aeolian Sand and Sand Dunes*. Unwin Hyman, London.
- Roberts, D. A., et al, 1998, "Mapping Chaparral in the Santa Monica Mountains using multiple endmember spectral mixture models", *Remote Sensing of Environment* 65: 267-279.
- Smith, M. O., et al, 1990, "Vegetation in deserts: I. A regional measure of abundances from multispectral images", *Remote Sensing of Environment* 31:1-26.
- Sohn, Y., and McCoy, R. M., 1997, "Mapping desert shrub rangeland using spectral unmixing and modeling spectral mixtures with TM data", *Photogrammetric Engineering and Remote Sensing* 63(5): 707-716.
- Stokes, S., and Swinehart, J. B., 1997, "Middle and Late Holocene dune reactivation in the Nebraska Sand Hills, USA", *The Holocene* 7: 263-272.
- USDA, 1968, *Soil Survey of Morgan County, Colorado*, USDA, Soil Conservation Service
- van Leeuwen, W.J.D. and A. R. Huete, 1996, "Effect of standing litter on the biophysical interpretation of plant canopies with spectral indices", *Remote Sensing of Environment*, 55(2): 123-138.